THE JOURNAL OF PHYSICAL CHEMISTRY B LETTERS

2006, *110,* 10602−10605
Published on Web 05/13/2006

Changes in Thermodynamic Interactions at Highly Immiscible Polymer/Polymer Interfaces due to Deuterium Labeling

Shane E. Harton,[†] Frederick A. Stevie,[‡] Zhengmao Zhu,[‡] and Harald Ade*[,§]

Department of Materials Science & Engineering, Analytical Instrumentation Facility, and Department of Physics, North Carolina State University, Raleigh, North Carolina 27695

Received: March 23, 2006; In Final Form: April 30, 2006

Deuterium labeling has been shown previously to affect thermodynamic interactions at polymer surfaces, polymer/polymer heterogeneous interfaces, and in bulk (away from a surface or interface). However, the changes in polymer−polymer interactions due to deuterium labeling have not been thoroughly investigated for highly immiscible systems. It is shown here that deuterium labeling can influence polymer−polymer interactions at heterogeneous interfaces with highly immiscible systems, namely, polystyrene/poly(2-vinylpyridine) (PS/P2VP), polystyrene/poly(4-vinylpyridine) (PS/P4VP), and polystyrene/poly(methyl methacrylate) (PS/PMMA). Using secondary ion mass spectrometry, segregation of deuterium labeled polystyrene (dPS) in a dPS + unlabeled PS (dPS:hPS) blend layer was observed at the dPS:hPS/hP2VP, dPS:hPS/hP4VP, and dPS:hPS/hPMMA heterogeneous interfaces. However, a reference system involving PS on a PS brush shows no segregation of dPS to the interface.

Polymer blend phase behavior can often be described in terms of a mean-field interaction parameter (χ).[1] For values of $\chi \leq 0$, a binary blend is completely miscible, and weak to moderate incompatibility will occur for $\chi \sim 0.001-0.01$, where miscibility windows are still readily available. However, for highly incompatible blends ($\chi > 0.1$) such as polystyrene/poly(2-vinylpyridine) (PS/P2VP)[2] and polystyrene/poly(4-vinylpyridine) (PS/P4VP),[3] miscibility windows are only achievable with very low molecular weight constituents (oligomers), if achievable at all. Increased control over the properties of incompatible polymers[4,5] has led to significant advances in the emerging fields of bio- and nanotechnology.[6] These advances have been greatly aided by the fundamental understanding brought about with improvements in characterization methods.[6,7] Many of these methods, including small angle neutron scattering (SANS), neutron reflectometry (NR), forward recoil spectrometry (FRES), nuclear reaction analysis (NRA), and secondary ion mass spectrometry (SIMS), utilize deuterium labeling in order to provide enhanced contrast for proper experimental characterization.[8,9]

Deuterium labeling involves replacing protium (^{1}H) in a compound (organic or inorganic) with its isotopic analogue (^{2}H). Although this method of labeling seems simple and unobtrusive, it has been shown to have a small, albeit finite, impact on polymer interactions at polymer surfaces,[10,11] polymer/polymer heterogeneous interfaces,[12] and in bulk (away from a surface or interface),[13,14] but these effects have not been thoroughly investigated with highly immiscible systems. Here, we show that effects of deuterium labeling on polymer−polymer interactions are also readily observable in highly immiscible polymer blends ($\chi \gg 0.01$). Three model systems, PS/P2VP, PS/P4VP, and polystyrene/poly(methyl methacrylate) (PS/PMMA),[12] show segregation of deuterium labeled PS (dPS) to the heterogeneous polymer/polymer interfaces. However, a reference system involving PS on a PS brush[15] shows no segregation of dPS to the interface. The PS/P2VP, PS/P4VP, and PS/PMMA systems have been previously utilized in many technologically relevant investigations, including polymer blending,[2,3,16] reactive compatibilization,[17−19] and tailoring of block copolymer morphology for directed nanoassembly.[15,20−23] Therefore, the findings presented here will provide an increased understanding of the effects of deuterium labeling on polymer phase behavior as well as improved characterization using techniques such as SANS, NR, FRES, NRA, and SIMS.

All polymers used in this investigation were purchased from Polymer Source or Scientific Polymer Products. Their chemical structures are listed in Figure 1. For the remainder of the paper, isotopic labeling will be distinguished with an *h* or *d* to signify specific unlabeled or deuterium labeled polymers, respectively. Differential scanning calorimetry was used to determine the glass transition temperatures (T_g), while thermogravimetric analysis was used to determine the degradation temperatures (T_d). Silicon (100) wafers were cut to 2.5 cm × 2.5 cm squares and cleaned in Baker Clean JTB-111 (J.T. Baker) and washed with deionized (DI) water. They were then etched with 10% (v/v) aqueous hydrofluoric acid, washed in DI water, and blown dry with N_2, thereby providing a hydrogen-passivated substrate (SiH). To prevent thermal degradation during the long annealing times used here, 3% (w/w on a solvent free basis) Irganox 1010 (Ciba-Geigy) was added to all polymers. Irganox 1010 has been shown to have a negligible surfactancy effect (i.e., preferential segregation) in polymer films.[24] hPMMA (M_n = 1490 kDa; M_w/M_n = 1.05; T_g = 130 °C; T_d = 360 °C), hP2VP (M_n = 1110 kDa; M_w/M_n = 1.10; T_g = 100 °C; T_d = 390 °C), and hP4VP

* Corresponding author. E-mail: harald_ade@ncsu.edu.
[†] Department of Materials Science & Engineering.
[‡] Analytical Instrumentation Facility.
[§] Department of Physics.

10.1021/jp061811d CCC: $33.50

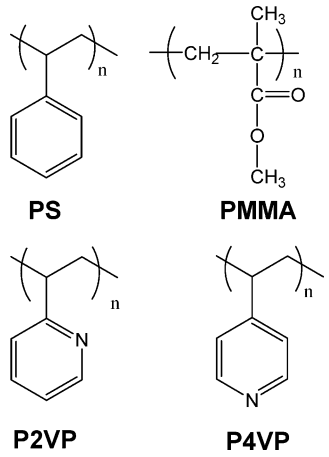

Figure 1. Chemical structures of the polymers used in this investigation.

(M_n = 94.6 kDa; M_w/M_n = 2.25; T_g = 150 °C; T_d = 360 °C) were all cast onto the SiH substrates from chlorobenzene or pyridine to a thickness ≈200 nm and annealed at 176 °C for 18 h. For production of an hPS brush,[15] SiH wafers were exposed to UV-ozone for 30 min to produce a native oxide layer ($SiO_x \approx 2$ nm), and hP(S-*b*-2VP) was cast from chlorobenzene onto the substrate. These samples were annealed for 18 h at 176 °C and subsequently washed with chlorobenzene, thereby producing a 10 nm hPS brush ($Z^*/R_g \approx 1.6$, where Z^* is the brush height, and R_g is the gyration radius of the hPS block),[15] as determined using ellipsometry. Thick PS layers (∼1.1 μm), containing 10% (v/v) dPS (M_n = 1500 kDa; M_w/M_n = 1.3; T_g = 100 °C; T_d = 400 °C) + 90% hPS (M_n = 1530 kDa; M_w/M_n = 1.03; T_g = 100 °C; T_d = 400 °C), were cast from toluene onto the hP2VP and hP4VP layers and the hPS brush. For production of the hPS:dPS/hPMMA films, the PS layer was cast onto SiO_x, scored with a sharp tip, floated into DI water, and picked up with the hPMMA layer. All samples were then placed in a vacuum at 176 °C for 64 days.

The dPS depth profiles were acquired using a CAMECA IMS-6f magnetic sector spectrometer.[25] The analysis conditions involved a 50 nA O_2^+ primary beam with a 5.5 keV impact energy that was rastered over a 180 μm × 180 μm area. Positive secondary ions were detected from a 60 μm diameter optically gated area at the center of the raster crater. The use of O_2^+ primary ion bombardment with detection of positive secondary ions was implemented in order to minimize sample charging of these thick insulating films.[26] A mass resolution ($m/\Delta m$) of 1250 was used to completely separate ^2H from $^1H_2$ while maintaining a high detection sensitivity.[25] Before the bilayers were depth profiled, a 70 nm (approximate) hPS sacrificial layer was floated onto the sample surface to ensure uniform sputtering rates and secondary ion yields before the start of the hPS:dPS layer. A 20 nm conductive Au coating was deposited on top of the sacrificial layer to further prevent charge buildup.[27] At least two spots were analyzed on each sample to ensure reproducibility of the depth profiles. The PS depth profiling rate (0.57 nm/s) was calibrated from three hPS:dPS/hPS brush profiles after measurement of the crater depths using profilometry.[25]

Measurement of the unconvoluted surface concentration of dPS (φ_s) for each sample (no sacrificial layer) was performed using time-of-flight (ToF) SIMS[28] with a PHI TRIFT I ToF mass spectrometer. The analysis conditions included a 15 keV Ga^+ primary ion energy with detection of positive secondary ions. A 600 pA primary ion current was used over a 100 μm × 100 μm detection area with a 7.2 kV extraction voltage. Charge neutralization was accomplished with a pulsed low energy electron beam (∼24 eV). The data acquisition time was set to 7 min, resulting in a total ion fluence of ∼5 × 10^{11} ions/cm^2 per analysis. Because this is below the so-called static limit, analysis was constrained to the top monolayer (<1 nm) of the film assembly.[29] Mass spectra were collected from three to four different spots on each sample and were subsequently analyzed using WinCadence software.

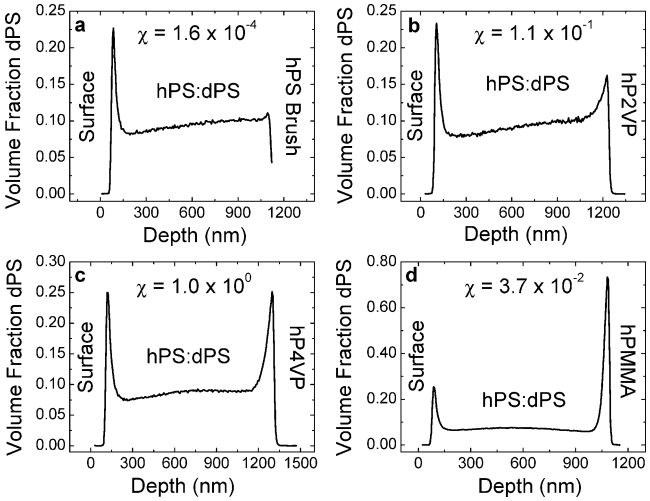

Figure 2. Depth profiling results for the (a) hPS:dPS/hPS brush, (b) hPS:dPS/hP2VP, (c) hPS:dPS/hP4VP, and (d) hPS:dPS/hMMMA blends. The previously reported χ values[2,3,13,14] between dPS and the bottom layer are also shown. It is quite clear from the diffusion gradient near the hPS:dPS surfaces and hPS:dPS/hPMMA interface that the systems are not at complete equilibrium, even after 64 days at 176 °C.

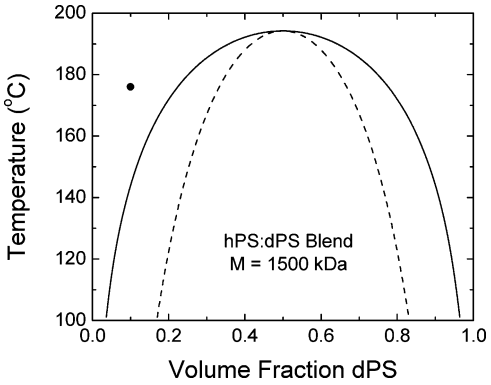

Figure 3. Phase diagram for a 1500 kDa symmetric hPS:dPS blend, as generated using parameters reported in ref 13 ($\chi = 0.20/T - 2.9 \times 10^{-4}$). The solid line is the binodal (coexistence curve), while the dashed line is the spinodal. The experimental temperature (T = 176 °C) and initial dPS volume fraction (0.1) is also shown (●).

After annealing for 64 days at 176 °C under vacuum, the samples were analyzed using SIMS, with the respective dPS depth profiles shown in Figure 2. Segregation of dPS is observed at all interfaces (see Figure 2), except the hPS:dPS/hPS brush interface (Figure 2a). Figure 3 shows that the hPS:dPS blend with 10% dPS (v/v) at 176 °C is within the single-phase region of the phase diagram,[13] and therefore, the observed segregation is not due to bulk phase separation of the hPS:dPS blend.[10] Negligible dPS segregation at the hPS:dPS/hPS brush interface confirms that variable dPS segregation at the heterogeneous polymer/polymer interfaces is not entropically driven (e.g., driven by polydispersity effects[30]), nor is it an artifact of sample preparation (i.e., dPS diffusion is strictly *to* a surface or interface from a homogeneous hPS:dPS blend and not *from* a surface or interface), and this control experiment eliminates any influence

TABLE 1: Surface Concentration of dPS for Each Sample as Determined Using ToF SIMS

bottom layer	φ_s
hPS brush	0.35
hP2VP	0.34
hP4VP	0.37
hPMMA	0.31

of the SiH or SiO_x substrates on the strength of the observed segregation. It is also shown that the segregation of dPS to the hPS:dPS surfaces (Figure 2) and the hPS:dPS/hPMMA interface (Figure 2d) are strongly diffusion-controlled,[10,12] implying that the enthalpic preference for dPS over hPS is greater than kT (thermal energy) per chain at these locations.[12] The diffusion gradient at the hPS:dPS surfaces and hPS:dPS/hPMMA interface (Figure 2) demonstrates that the diffusive flux (chemical potential gradient) favors an increase in dPS segregation to the hPS:dPS surfaces and hPS:dPS/hPMMA interface.[10,31] The lack of a gradient at the hPS:dPS/hPS brush, hPS:dPS/hP2VP, and hPS:dPS/hP4VP interfaces (Figure 2a−c) shows that the dPS segregation strength is weaker ($<kT$ per chain), or nonexistent in the case of the hPS:dPS/hPS brush interface, for these systems than with the hPS:dPS/hPMMA system.[12] Because there is no driving force for reversal of the observed segregation under these constant experimental conditions, the observed segregation in Figure 2 can be considered a lower limit of the equilibrium amounts.[10]

Theoretical analysis of equilibrium segregation of dPS to an hPS:dPS surface further confirms that the observed segregation for all systems shown in Figure 2 is indeed a lower limit. Using a previously reported model and parameters,[10] a surface volume fraction of dPS (φ_s) of approximately 0.75 for the system and experimental conditions implemented here is expected. Experimental analysis of φ_s using ToF (static) SIMS[28] reveals much lower surface compositions than theoretically predicted, as shown in Table 1. However, the enthalpic preference for dPS over hPS at a heterogeneous interface can be ordered, from strongest to weakest, as the hPS:dPS/hPMMA interface ($\sim 1 \times 10^{-2} kT$ per segment),[12] hPS:dPS/hP4VP interface ($>2 \times 10^{-3} kT$ per segment), and hPS:dPS/hP2VP interface ($>1 \times 10^{-3} kT$ per segment). The lower limits for the dPS enthalpic preference at the hPS:dPS/hP4VP and hPS:dPS/hP2VP interfaces were approximated from the square-gradient model described in ref 10.

Figure 2 also shows the previously reported values for χ between dPS and hPS (Figure 2a),[13] dPS and hP2VP (Figure 2b),[2] dPS and hP4VP (Figure 2c),[3] and dPS and hPMMA (Figure 2d).[14] According to mean-field theory, the enthalpic preference for dPS at the interface can be approximated by[32,33]

$$\Delta\chi_p \cong \lambda_1(\chi_{h,b} - \chi_{d,b}) \sim 2\lambda_1(\chi_{h,d}\chi_{d,b})^{1/2} \qquad (1)$$

where $\Delta\chi_p$ is the enthalpic preference for a dPS segment at the heterogeneous interface (scaled to kT),[12] $\chi_{h,d}$ is the mean-field interaction parameter for hPS and dPS, $\chi_{d,b}$ is the interaction parameter for dPS and the bottom layer polymer, $\chi_{h,b}$ is the interaction parameter for hPS and the bottom layer polymer, and λ_1 is a weighting factor (1/6 for a cubic lattice).[32] In deriving eq 1 (far right side), it was assumed that $\chi_{h,b} = (\chi_{d,b}^{1/2} + \chi_{h,d}^{1/2})^2$ (geometric mean approximation)[33] and the bottom layer polymer has a more favorable interaction with dPS than with hPS, which is experimentally observed in Figure 2b−d. Equation 1 does predict the correct order of magnitude for $\Delta\chi_p$ for the hPS:dPS/hP2VP and hPS:dPS/hP4VP interfaces, but it predicts a $\Delta\chi_p$ value that is over an order of magnitude *lower* than the experimentally determined $\Delta\chi_p$ for the hPS:dPS/hPMMA interface.[12] Also, although a monotonic increase in $\Delta\chi_p$ should be observed with an increase in $\chi_{d,b}$ at constant $\chi_{h,d}$, there is no clear relationship between the values of $\chi_{d,b}$ and the strength of dPS segregation observed here. Because the influence of the bottom layer on the degree of dPS segregation cannot be related to the bulk phase behavior ($\chi_{d,b}$), the observed changes in interactions at polymer/polymer heterogeneous interfaces due to isotopic labeling may not be consistent with current mean-field theories.[12,34] The underlying mechanism and relevant parameters behind these varying degrees of segregation are unknown at this time, and future work should indeed focus on the molecular level mechanisms behind this macroscopically observed phenomenon.[13]

In conclusion, we have observed segregation of dPS to heterogeneous polymer/polymer interfaces from hPS:dPS blends using model PS/P2VP,[2] PS/P4VP,[3] and PS/PMMA[12,14] systems. This confirms that deuterium substitution can affect polymer−polymer interactions at interfaces between highly incompatible polymers. Because deuterium labeling is often employed in order to experimentally characterize phenomena such as polymer blending[2,3,16] and reactive compatibilization,[17−19] improved understanding and predictive capabilities into the effects of deuterium labeling is technologically relevant. However, the relative strength of these effects could not be predicted using the independently determined mean-field interaction parameter (χ) between dPS and the bottom layer polymer (see eq 1), and as such, future work should focus on the molecular level mechanisms and relative parameters behind the observed segregation phenomenon.

Acknowledgment. This work was supported by the U. S. Department of Energy (DE-FG02-98ER45737).

References and Notes

(1) Flory, P. J. *Principles of Polymer Chemistry*; Cornell University Press: Ithaca, NY, 1953.

(2) Dai, K. H.; Kramer, E. J. *Polymer* **1994**, *35*, 157.

(3) Clarke, C. J.; Eisenberg, A.; LaScala, J.; Rafailovich, M. H.; Sokolov, J.; Li, Z.; Qu, S.; Nguyen, D.; Schwarz, S. A.; Strzhemechny, Y.; Sauer, B. B. *Macromolecules* **1997**, *30*, 4184.

(4) Ryan, A. J. *Nat. Mater.* **2002**, *1*, 8.

(5) Ruzette, A. V.; Leibler, L. *Nat. Mater.* **2005**, *4*, 19.

(6) Granick, S.; Kumar, S. K.; Amis, E. J.; Antonietti, M.; Balazs, A. C.; Chakraborty, A. K.; Grest, G. S.; Hawker, C.; Janmey, P.; Kramer, E. J.; Nuzzo, R.; Russell, T. P.; Safinya, C. R. *J. Polym. Sci., Part B: Polym. Phys.* **2003**, *41*, 2755.

(7) Harton, S. E.; Stevie, F. A.; Zhu, Z.; Ade, H. *Anal. Chem.*, in press.

(8) Kramer, E. J. *Physica B* **1991**, *173*, 189.

(9) Roe, R.-J. *Methods of X-ray and Neutron Scattering in Polymer Science*; Oxford University Press: New York, 2000.

(10) Jones, R. A. L.; Kramer, E. J.; Rafailovich, M. H.; Sokolov, J.; Schwarz, S. A. *Phys. Rev. Lett.* **1989**, *62*, 280.

(11) Hariharan, A.; Kumar, S. K.; Rafailovich, M. H.; Sokolov, J.; Zheng, X.; Duong, D. H.; Schwarz, S. A.; Russell, T. P. *J. Chem. Phys.* **1993**, *99*, 656.

(12) Harton, S. E.; Stevie, F. A.; Ade, H. *Macromolecules* **2006**, *39*, 1639.

(13) Bates, F. S.; Wignall, G. D. *Phys. Rev. Lett.* **1986**, *57*, 1429.

(14) Russell, T. P. *Macromolecules* **1993**, *26*, 5819.

(15) Segalman, R. A.; Hexemer, A.; Kramer, E. J. *Phys. Rev. Lett.* **2003**, *91*, Art. No. 196101.

(16) Russell, T. P.; Anastasiadis, S. H.; Menelle, A.; Felcher, G. P.; Satija, S. K. *Macromolecules* **1991**, *24*, 1575.

(17) Harton, S. E.; Stevie, F. A.; Ade, H. *Macromolecules* **2005**, *38*, 3543.

(18) Schulze, J. S.; Cernohous, J. J.; Hirao, A.; Lodge, T. P.; Macosko, C. W. *Macromolecules* **2000**, *33*, 1191.

(19) Kim, B. J.; Kang, H.; Char, K.; Katsov, K.; Fredrickson, G. H.; Kramer, E. J. *Macromolecules* **2005**, *38*, 6106.

(20) Lin, Y.; Boker, A.; He, J. B.; Sill, K.; Xiang, H. Q.; Abetz, C.; Li, X. F.; Wang, J.; Emrick, T.; Long, S.; Wang, Q.; Balazs, A.; Russell, T. P. *Nature* **2005**, *434*, 55.

(21) Mansky, P.; Liu, Y.; Huang, E.; Russell, T. P.; Hawker, C. *Science* **1997**, *275*, 1458.

(22) Ruokolainen, J.; Mäkinen, R.; Torkkeli, M.; Mäkelä, T.; Serimaa, R.; ten Brinke, G.; Ikkala, O. *Science* **1998**, *280*, 557.

(23) Kim, B. J.; Chiu, J. J.; Yi, G. R.; Pine, D. J.; Kramer, E. J. *Adv. Mater.* **2005**, *17*, 2618.

(24) Médard, N.; Poleunis, C.; Vanden Eynde, X.; Bertrand, P. *Surf. Interface Anal.* **2002**, *34*, 565.

(25) Harton, S. E.; Stevie, F. A.; Ade, H. *J. Vac. Sci. Technol., A* **2006**, *24*, 362.

(26) Parks, C. C. *J. Vac. Sci. Technol., A* **1997**, *15*, 1328.

(27) Pivovarov, A. L.; Stevie, F. A.; Griffis, D. P. *Appl. Surf. Sci.* **2004**, *231*−*232*, 786.

(28) Affrossman, S.; Hartshorne, M.; Jerome, R.; Munro, H.; Pethrick, R. A.; Petitjean, S.; Vilar, M. R. *Macromolecules* **1993**, *26*, 5400.

(29) Wilson, R. G.; Stevie, F. A.; Magee, C. W. *Secondary Ion Mass Spectrometry: A Practical Handbook for Depth Profiling and Bulk Impurity Analysis*; John Wiley & Sons: New York, 1989.

(30) Broseta, D.; Fredrickson, G. H.; Helfand, E.; Leibler, L. *Macromolecules* **1990**, *23*, 132.

(31) Geoghegan, M.; Nicolai, T.; Penfold, J.; Jones, R. A. L. *Macromolecules* **1997**, *30*, 4220.

(32) Fleer, G. J.; Stuart, M. A. C.; Scheutjens, J. M. H. M.; Cosgrove, T.; Vincent, B. *Polymers at Interfaces*; Chapman & Hall: New York, 1993.

(33) Hariharan, A.; Kumar, S. K.; Russell, T. P. *J. Chem. Phys.* **1993**, *98*, 6516.

(34) Feng, E. H.; Fredrickson, G. H. *Macromolecules* **2006**, *39*, 2364.